Dye Lasers in COMSOL

Student: Passarelli Nicolás

Universidad de Málaga, Av. De Cervantes, 2, 29016, Málaga

Tutor: Emilio Ruiz Reyna

Universidad de Málaga, Av. De Cervantes, 2, 29016, Málaga

Abstract. In this master thesis, the author boarded the computational implementation, on the software COMSOL Multiphysics, for the physics of dye Lasers. This physics is a semi-classical formalism in which the dye is represented as a set of discrete states, typically four, populated by electrons. The transitions between these states can be spontaneous or stimulated, and both kinds depend on the population of the two levels involved in the transition. These transitions are associated with a polarization response and to currents. The formalisms to describe this was developed originally for the finite differences in the time domain. For this master thesis, the original results were reproduced, validating the physics in the finite elements methods native on COMSOL.

I. INTRODUCTION

A.Motivation

The student proposed this work because he aims to become an expert in lasing. He is a young researcher who entered the world of nano-optics in his PhD and was the first to write articles on plasmonic nanolasers in Argentina, his natal country. He proposed several devices solved analytically[1-3]. In these works, the lasing conditions are found despite the impossibility of solving the gain media dynamics; thus, lasing is probed but is not described correctly. On his postdoc in Spain, he participated in a project in which a photonic crystal dye laser was built experimentally. The match between experiments and simulations could be done with the four-level two-electrons model, implemented in a very established software for photonics[4]. This work is to be published soon. This experience served to know the model, its limitations, and the limitations of implementing it in a suite just for photonics. COMSOL offers the possibility to link dye physics to another, which is the motivation for the present work.

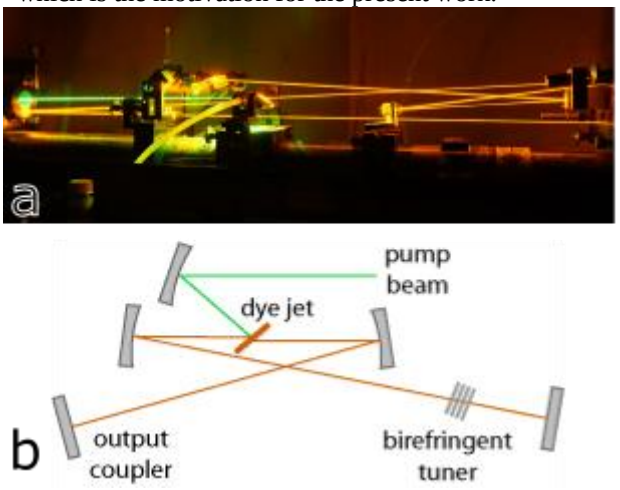

FIG. 1: a) Dye laser photo (creative commons BY-SA 4.0).
b) scheme (taken from webpage https://www.rp-photonics.com/previews/dye_lasers.png)

B. Antecedents

Between 1916 and 1917, Albert Einstein took Max Planck's formalism and posed the electrodynamic equations for a new phenomenon: the stimulated emission of radiation. However, until 1953, Charles H. Townes experimentally demonstrated the feasibility of microwave stimulated emission. Then, in 1962 it was brought into the visible region of the spectrum with the first ruby LASER, which stands for Light Amplification by Stimulated Emission of Radiation[5]. A scientific-technical revolution is unleashed thanks to this. Intensities and coherence were reached at unprecedented levels, availing the development of new spectroscopic techniques, microscopies, and optical phenomena. Today, lasers are used for communication, surgery, data reading and storage, ultrasensitive detection, and security systems, among other applications.

The core of any kind of laser is the active media, a material that can provide the stimulated emission. For this purpose, it must have discrete energy levels or bands that sustain transitions, and the higher energy state of a transition must hold a bigger population than the lowest. For this to happen, an efficient pumping method must be implemented. The laser must provide an optical mode, typically a cavity mode, with the same frequency that the transition. In this way, the mode is amplificated by the stimulated emission.

Semiconductor lasers (SL) or diode lasers are a type of solid-state lasers that are the most broadly used. In these SLs, a forward electrical bias across the p–n junction that forms the diode creates an area with excess electrons and holes. These electrons and holes can recombine with the release of energy in photons; this recombination can be spontaneous or stimulated by another photon. Spontaneous emission is used in light-emitting diodes (LED), while stimulated emission is the basis for either superluminescent diodes or laser diodes[6]. Most SLs are laser diodes pumped with an electrical current near the region where n-doped and p-doped semiconductor material meet. However, there are also optically pumped semiconductor lasers generated by

absorbed pump light and quantum cascade lasers, in which intraband transitions are utilized[7].

Great care has to be taken that the crystal used for a semiconductor laser has almost perfect quality. In detail, dislocations in the crystal have to be avoided and any kinds of defects since they act as nonradiative recombination centres. Choosing a laser material for a specific desired wavelength range thus implies two critical requirements: first, the bandgap of the material has to fit the desired photon energy and second, and more severe, a substrate with the right lattice constant has to be found[8].

Unlike semiconductors, atoms, molecules, biomolecules, complexes, and quantum dots have an electronic structure that can provide stimulated emission. Still, they are not restricted to the solid state, and their emission can be engineered chemically.

With these elements, one can cover the photonic region of the electromagnetic spectra. Organic dye molecules can offer electronic transitions with ultraviolet and visible region emissions. Some metal complexes also emit in the visible. Depending on composition and size, quantum dots do it in the range from the visible to the near-infrared; In this latter region, heavy atoms' electronic transitions can also operate. Gas-phase small molecules provide vibrational transitions among the IR, and recently stimulated Raman scattering was reported for doped silicon on the terahertz[9]. Although this thesis is dedicated to dyes lasers, all these systems can be modelled with the same physics.

Tipically, dyes are four-level quantum systems, and the transitions occur between the electronic levels modified strongly by molecular vibrations. The interactions between electrons and molecular vibrations, called *vibronic coupling*, lead to the band-broadening of the absorption and emission lines[11]. Pump transition is from the ground-vibrational of the lower electronic state S_0, to an excited electronic S_1 and vibronic; marked with (1) in figure 2. Then the state quickly relaxes to the ground vibrational of S_1 (2). The emission, ad lasing, occurs to an excited state of the lower electronic level (3), followed by another relaxation to the ground of S_0 (4).

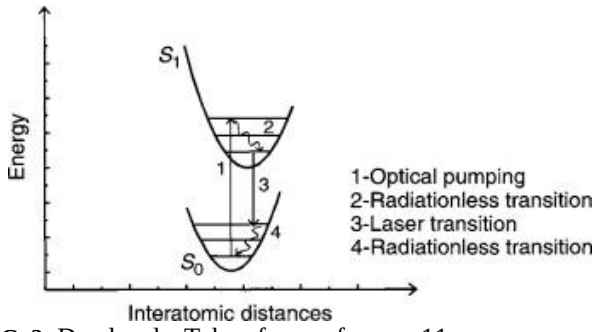

FIG. 2: Dye levels. Taken from reference 11.

Dye lasers (DyL) were discovered in 1966 by Fritz P. Schäfer et al.; they are similar to solid-state lasers due to they consist of a host material, in this case a solvent. The main difference is that dyes are pumped optically, one year after the discoverers managed to pump effectively with a flashlamp. Different coloured molecules have different emission spectra or colours and a broad emission spectrum (typically 30–60 nm) over which gain occurs[10]. These broad emission spectra give them their characteristic tunability. For example, one can control the emission frequency by changing the cavity mode with a birefringent crystal or diffraction grating. In figure 1 one can see a photograph of a dye laser, in which one can see two beams the pumping (green laser) and the emitted by the dispositive (orange).

Tunability is used either to select a specific frequency that is not available from one of the solid-state or gas lasers or to study the properties of a material when the laser frequency is varied over a wide range. Broad emission spectra also offer the possibility of mode-locking or phase-locking; it is interference between a vast number of optical modes amplified under the emission bell, causing a train of intense pulses. In this way, Dye lasers can be continuous or pulsed.

Most dye lasers are arranged to have the solution circulated into the gain region from a more extensive reservoir since these organic molecules degrade slightly during the excitation process. In figure 1a, one can see the hose with the liquid. Moreover, this design also allows changing the molecule or using mixes without changing the resonator. In this sense, DyLs are more versatile than SL for general purposes.

In the last decade, lasers physic began to be sought in devices at the micro and nano-scale[12]. These super-intense sources of coherent radiation promise to replace the macroscopic laser for implementation in more energy-efficient, faster and portable devices. There are five main kinds of small-scale laser: SPASERs (Surface Plasmon Amplification by Stimulated Emission of Radiation), plasmonic nanolasers, nanowire lasers, photonic crystal lasers and vertical-cavity surface-emitting lasers (VCSEL)[13]. Surface plasmons of metals, which are evanescent waves confined to the surface of metals, play an important role because they can create huge confinements.

In both plasmonic and non-plasmonic devices, the key is to generate electromagnetic densities that can be several times that of the incoming light, favouring stimulated transitions. Moreover, when the device's size is in the order of magnitude of the wavelength, the number of optical modes available is drastically reduced; fewer output channels are competing. For generating lasing, the gain media must compensate for the losses of the amplificated mode, both radiative and Ohmic (heating), which can be critical in metals[14]. Optically pumped SPASERs performances are particularly sensitive to the heat generated

by its functioning, including the thermal release from the metal and also from the dye [15].

Figure 3 shows a selection of nano-DyLs to illustrate the different mechanisms for lasing that can be attained with dyes. In examples a) b) and c) fluidics was exploted for dyes in the dissolved phase; in the others, these molecules are hosts in a polymeric matrix, giving mechanical sustain to the device. Panels d) and e) shows examples of non-plasmonic lasers, whereas a) uses propagating plasmons, b) cavity modes and whispering gallery modes, c) plasmon lattice resonances and f) localized surface plasmons.

For this master thesis, the case of the VCSEL will be boarded in deep. Typically, the gain medium is sandwiched between two distributed Bragg reflectors (DBRs) in this kind of laser. These reflectors work as dielectric mirrors blocking light of a wide range of wavelengths without generating appreciable amounts of heat. The gain is hosted in a cavity that provides a localized mode. The power density of this mode is concentrated in the gain media (more in figure 4), and its frequency becomes the frequency of the output amplificated radiation.

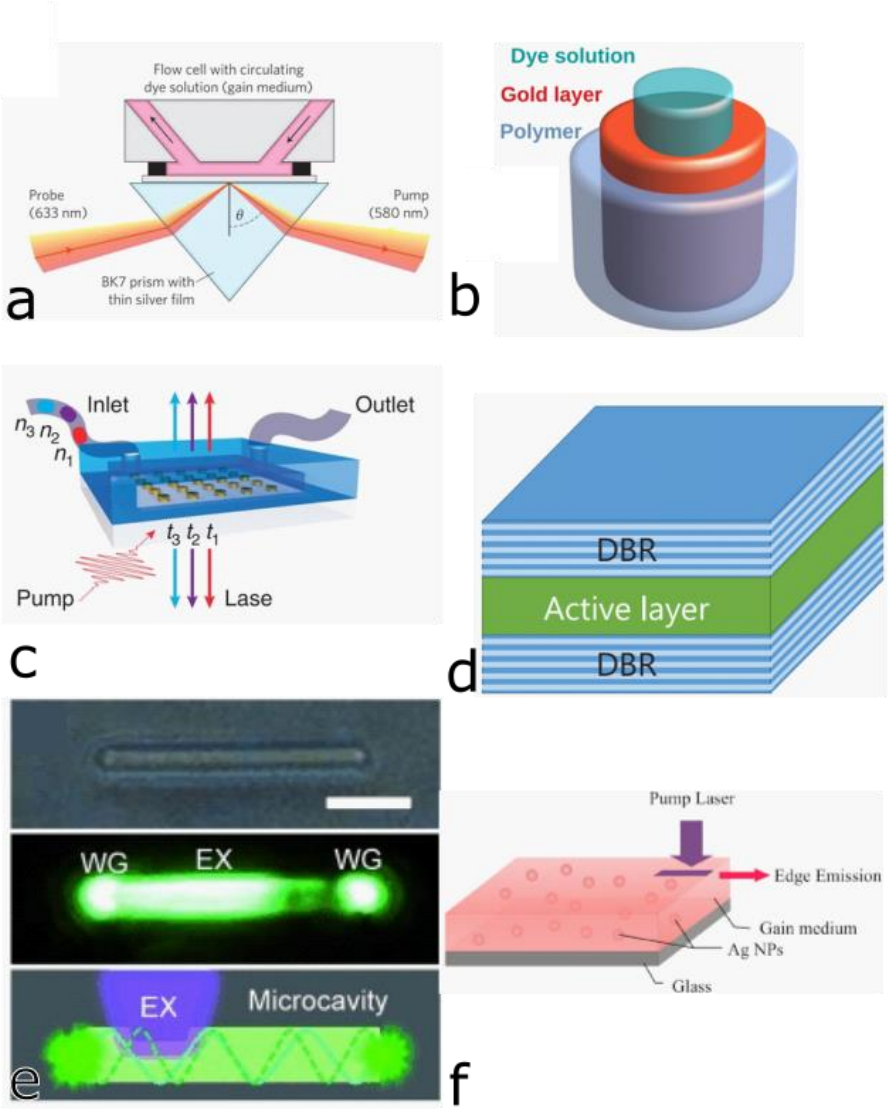

FIG. 3: Examples of nano dye lasers of different kinds **a)** SPASER[16]. **b)** Nanotube Laser[2]. **c)** Photonic crystal[17]. **d)** VCSEL [18] **e)** Nanowire laser[19]. **f)** Nanoparticle SPASER [20]

II. THEORY

A. Electromagnetic formulation

Maxwell equations rule Electromagnetism in the matter. They are two different conventions to these equations; in this thesis, we will consider the international system (SI) convention (equations 1 to 4), and SI units.

$$\nabla\cdot\mathbf{D} = \rho_f \quad (1)$$

$$\nabla\cdot\mathbf{B} = 0 \quad (2)$$

$$\nabla\times\mathbf{E} = -\frac{\partial \boldsymbol{B}}{\partial t} \quad (3)$$

$$\nabla\times\mathbf{H} = \boldsymbol{J}_f + \frac{\partial \boldsymbol{D}}{\partial t} \quad (4)$$

$\boldsymbol{E}$ and $\boldsymbol{B}$ are the electric and magnetic vector fields (vector fields are in bold). ρ and $\boldsymbol{J}$ are the charge density (total charge per unit of volume) and the total current density (current per unit of area), the subscript 'f' refers to free charge carriers, those that can circulate. $\boldsymbol{D}$ is the displacement field, and $\boldsymbol{H}$ is the magnetizing field. The latter two are related to $\boldsymbol{E}$ and $\boldsymbol{B}$ through the auxiliary fields:

$$\mathbf{D} = \varepsilon_0\boldsymbol{E} + \boldsymbol{P} \quad (5)$$

$$\boldsymbol{H} = \frac{1}{\mu_0}\boldsymbol{B} - \boldsymbol{M} \quad (6)$$

Where $\boldsymbol{P}$ and $\boldsymbol{M}$ are the polarization and magnetization of the material. ε_0 and μ_0 are the electric permittivity and magnetic permeability of free space, which are related to its light velocity $c_0 = (\varepsilon_0\mu_0)^{-1/2}$ .The polarization and magnetization have two general terms: one permanent, which applies to electrects and magnets, and one induced. The induced polarization and magnetization are related to the electric and magnetic fields through the constitutive relations. These relations can be generalized as taylor expansions, introducing electric and magnetic susceptibilities χ, as shown in equations 7 and 8. In general materials can be anisotropic, so these susceptibilities need to be considered tensors.

$$\boldsymbol{P}_{\boldsymbol{induced}} = \varepsilon_0\chi_e^{(1)}\boldsymbol{E} + \varepsilon_0\chi_e^{(2)}\boldsymbol{E}^2 + \varepsilon_0\chi_e^{(3)}\boldsymbol{E}^3 \ldots \quad (7)$$

$$\boldsymbol{M}_{\boldsymbol{induced}} = \chi_m^{(1)}\boldsymbol{B} + \chi_m^{(2)}\boldsymbol{B}^2 + \chi_m^{(3)}\boldsymbol{B}^3 \ldots \quad (8)$$

Equations 1 to 8 are the most general form of electromagnetism equations. Still, in most cases, one is dealing with particular systems, and generalities can be precluded to simplify the equations. The materials boarded here are uncharged, and homogeneous. No electrects or magnets are considered, and linear induction for the electric and magnetic fields is enough for the physics studied. The electric permeability of the material is defined as $\varepsilon = \varepsilon_0\left(1+\chi_e^{(1)}\right)$. Similarly, one can define the magnetic permittivity $\mu = \mu_0\left(1+\chi_m^{(1)}\right)$. Because of these linearities, the relative quantities can be defined $\varepsilon_r = \varepsilon/\varepsilon_0$ and $\mu_r = \mu/\mu_0$.

Thus our simplified set of equations is (equations 9 to 12):

$$\varepsilon\nabla\cdot\mathbf{E} = 0 \quad (9)$$

$$\nabla\cdot\mathbf{B} = 0 \quad (10)$$

$$\nabla\times\mathbf{E} = -\frac{\partial \boldsymbol{B}}{\partial t} \quad (11)$$

$$\frac{1}{\mu}\nabla\times\mathbf{B} = \boldsymbol{J}_f + \varepsilon\frac{\partial \boldsymbol{E}}{\partial t} \quad (12)$$

When considering equation 10, a null divergence suggests that the magnetic field is the curl of a quantity $\boldsymbol{A}$, which is called the magnetic vector potential. Then, comparing with equation 11, one can deduce that $\mathbf{E} = -\frac{\partial \boldsymbol{A}}{\partial t}$. Putting it all together, one can find the following formulation from equation 12:

$$\nabla\times\mu_r^{-1}(\nabla\times\boldsymbol{A}) - \mu_0\boldsymbol{J}_f + \mu_0\frac{\partial}{\partial t}\left(\varepsilon_0\varepsilon_r\frac{\partial \boldsymbol{A}}{\partial t}\right) = 0 \quad (13)$$

Equation 13 is the formulation that will be finally used. The computational implementation finds $\boldsymbol{A}$ numerically, and from this, the fields are retrieved.

B. Wave modes

When considering the interface of two materials, one needs to consider boundary conditions. The border of material 1 and material 2 has a normal versor $\hat{n}_{12}$, with this versor one, the following boundary conditions can be written(equations 14 to 17):

$$\hat{n}_{12}\times(\boldsymbol{E}_2 - \boldsymbol{E}_1) = 0 \quad (14)$$

$$\hat{n}_{12}\cdot(\varepsilon_2\boldsymbol{E}_2 - \varepsilon_1\boldsymbol{E}_1) = 0 \quad (15)$$

$$\hat{n}_{12}\times\left(\frac{\mathbf{1}}{\boldsymbol{\mu_2}}\boldsymbol{B}_2 - \frac{\mathbf{1}}{\boldsymbol{\mu_1}}\boldsymbol{B}_1\right) = 0 \quad (16)$$

$$\hat{n}_{12}\cdot(\boldsymbol{B}_2 - \boldsymbol{B}_1) = 0 \quad (17)$$

Equations 14 and 15 are not the general case; instead of being null, they should equal the free surface charge density and the free surface current density, respectively.

The boundaries define the system, as the boundary conditions determine the solution to its electromagnetism. Maxwell equations are wave equations, and the interfaces confine the waves. Confinement splits the solution of wave equations into a set of eigenmodes and eigenfrequencies.

Only a few systems with particular geometries can be solved analytically. This limitation is because one needs to find a set of wavefunctions and boundary conditions compatible with the geometry. These solvable are planar and multi-stack layers, spheres and concentric spheres, cylinders and concentric cylinders. The rest need to be implemented numerically.

C. Four level two electrons model

As introduced above, the dye physics is complex. It cannot be described by a set of constant permittivity and permeability. The quantum dynamics of the four levels system were translated to the classical framework by Allen Taflove and implemented in the finite differences time domain in reference FDTD[21], which is crucial for this thesis.

Let N_0, N_1, N_2 and N_3 be the population probability density on each volume differential. We will consider these as four real numbers, given that they represent an average over a vast number of individual molecules with a population of zero or one. The transition between these states respects Pauli's exclusion principle: electrons cannot go to fully occupied states. Equations 18 to 21 are the rate equations for these four levels.

$$\frac{dN_0}{dt} = \frac{N_3(1-N_0)}{\tau_{30}} + \frac{N_1(1-N_0)}{\tau_{10}} + \frac{1}{\hbar\omega_b}\boldsymbol{E}\cdot\frac{d\boldsymbol{P_b}}{dt} \quad (18^*)$$

$$\frac{dN_1}{dt} = \frac{N_2(1-N_1)}{\tau_{21}} - \frac{N_1(1-N_0)}{\tau_{10}} + \frac{1}{\hbar\omega_a}\boldsymbol{E}\cdot\frac{d\boldsymbol{P_a}}{dt} \quad (19^*)$$

$$\frac{dN_2}{dt} = \frac{N_3(1-N_2)}{\tau_{30}} - \frac{N_2(1-N_1)}{\tau_{21}} - \frac{1}{\hbar\omega_a}\boldsymbol{E}\cdot\frac{d\boldsymbol{P_a}}{dt} \quad (20^*)$$

$$\frac{dN_3}{dt} = -\frac{N_3(1-N_2)}{\tau_{32}} - \frac{N_3(1-N_0)}{\tau_{30}} - \frac{1}{\hbar\omega_b}\boldsymbol{E}\cdot\frac{d\boldsymbol{P_b}}{dt} \quad (21^*)$$

In these equations, there are two kinds of terms: spontaneous transitions $N_i(1-N_j)/\tau_{ij}$, which have a lifetime τ_{ij}; and stimulated ones $\boldsymbol{E}\cdot\frac{d\boldsymbol{P_k}}{dt}/h\omega_k$, which have associated polarization density $\boldsymbol{P_k}$ and an angular frequency ω_k (the energy difference between the states divided by the reduced Plank constant $\hbar$). The subscript 'k' stands for 'a' or 'b', which are the transitions 2→1 and 0→3, respectively.

The 'a' and 'b' polarization densities are governed by equations 21 and 22. These transitions have a damping coefficient γ which stands for the nonradiative loss. In the equations are introduced the constants $\xi_k = 6\pi\varepsilon_0 c^3/\omega_k\tau_k$.

$$\frac{d^2\boldsymbol{P_a}}{dt^2} + \gamma_a\frac{d\boldsymbol{P_a}}{dt} + {\omega_a}^2\boldsymbol{P_a} = \xi_a(N_2-N_1)\boldsymbol{E} \quad (22)$$

$$\frac{d^2\boldsymbol{P_b}}{dt^2} + \gamma_b\frac{d\boldsymbol{P_b}}{dt} + {\omega_b}^2\boldsymbol{P_b} = \xi_b(N_3-N_0)\boldsymbol{E} \quad (23)$$

For the sake of clarity, one can solve these equations in the frequency domain. See equation 24. The polarization fades far from the frequency ω_k with a bandwidth given by the damping γ_k. Taking inverse Fourier, and neglecting contributions far from ω_k, one can obtain an approximation to its time domain expression and its derivative

$$\boldsymbol{P_k}(\omega) = \frac{\xi_k(N_j-N_i)}{{\omega_k}^2-\omega^2+i\gamma_k\omega}\boldsymbol{E}(\omega) \quad (24)$$

$$\boldsymbol{P_k}(t) = \frac{1}{2\pi}\int_{-\infty}^{\infty}\frac{\xi_k(N_j-N_i)}{{\omega_k}^2-\omega^2+i\gamma_k\omega}\boldsymbol{E}(\omega)e^{i\omega t}\,d\omega \simeq \frac{\xi_k(N_j-N_i)}{i\gamma_k\omega_k}\boldsymbol{E}(\omega_k)e^{i\omega_k t} \quad (25)$$

$$\frac{d\boldsymbol{P_k}(t)}{dt} \simeq \frac{\xi_k(N_j-N_i)}{\gamma_k}\boldsymbol{E}(\omega_k)e^{i\omega_k t} \quad (26)$$

Note that stimulated transitions are proportional to $(N_j-N_i)\boldsymbol{E}(\omega_k)\cdot\boldsymbol{E}(t)$. The squared electric field is proportional to the power, here we have an analogous term (projected over the mode of frequency 'k'). The population difference between the states determines whether the polarization is enforcing or weakening the fields. It is emitting or absorbing energy near ω_k.

Spontaneous transitions have the form $N_j(1-N_i)/\tau_{ij}$, it is proportional to the population of the initial state N_j and to the term $(1-N_i)$ that comes from Pauli's exclusion principle. The longer the lifetime, the slowest is the spontaneous transition.

The polarization densities generate currents that can be introduced in the Ampère-Maxwell law. Considering the total concentration of the dye N_{dye} these currents are:

$$\boldsymbol{J_a} = N_{dye}\frac{d\boldsymbol{P_a}}{dt} \quad (27)$$

$$\boldsymbol{J_b} = N_{dye}\frac{d\boldsymbol{P_b}}{dt} \quad (28)$$

$$\boldsymbol{J_f} = \boldsymbol{J_a} + \boldsymbol{J_b} \quad (29)$$

III. METHODS

The numerical implementation for solving the set of equations planted above was entirely done in COMSOL Multiphysics. The optics branch's 'Electromagnetic waves' modules can deal with the electromagnetic solutions. These modules are appropriate for the length scale of the system, which is the same as the wavelength. Equations 18 to 23 were implemented into two distributed ordinary equations nodes: one for the population dynamic (equations 17 to 21) and the other for the polarization densities.

The module offers three different formalisms: time-dependent, frequency-dependent and transient. The two former offer a built-in possibility to enter currents into the Ampère-Maxwell law. The frequency-domain cannot give the temporal evolution of interest, but it is useful to describe the system without the gain media. The time explicit formulation can neither solve non-linear media because it depends on time. In contrast, the transient method can deal with our four level two electron material, but it had to be modified to include the currents given by equations 27 to 29.

For the linear media the current is taken of the form $\boldsymbol{J_f} = \sigma\boldsymbol{E}$, where σ is the conductivity (null in our case, without metals).

$$\nabla\times\mu_r^{-1}(\nabla\times\boldsymbol{A}) + \mu_0\sigma\frac{\partial\boldsymbol{A}}{\partial t} + \mu_0\frac{\partial}{\partial t}\left(\varepsilon_0\varepsilon_r\frac{\partial\boldsymbol{A}}{\partial t}\right) = 0 \quad (30)$$

For the gain media the modified formulation for the electric wave equation is

$$\nabla\times\mu_r^{-1}(\nabla\times\boldsymbol{A}) + \mu_0\left(\sigma\frac{\partial\boldsymbol{A}}{\partial t} - N_{dye}\frac{d\boldsymbol{P_a}}{dt} - N_{dye}\frac{d\boldsymbol{P_b}}{dt}\right) + \mu_0\frac{\partial}{\partial t}\left(\varepsilon_0\varepsilon_r\frac{\partial\boldsymbol{A}}{\partial t}\right) = 0 \quad (31)$$

The main difficulty faced is the high computational cost of this model; simulations need to be very large. The electric field and the dye polarizations oscillate at optical frequencies, which is the order of $10^{14}Hz$. Thus, the characteristic time is about $10fs$; and, to get a proper discretization, the time steps must be below the femtosecond. On the other hand, the transitions have

[*] In reference 21 the signs of all stimulated terms are the opposite. There is an erratum of the reference; for this work, equations 18 to 21 are used as shown.

lifetimes typically on the nanoseconds, seven orders of magnitude bigger.

To reduce the simulation time, the time step must be fixed to one-eighth of the period of the pumping wave; in one eighth, just the maxima, minima and zeros of the wave are included, which are the principal features of the wave. The mesh has one cell of width since the mirror at normal incidence is a 1D problem (Optics formulations are available only in 2D and 3D). And finally, only the population N_1, N_2 and N_3 (equations 19 to 21) were solved, and N_0 was calculated from the conservation of electrons $N_0 = 2 - N_1 - N_2 - N_3$.

VI. RESULTS AND DISCUSSION

This thesis aims to develop a methodology that can be applied to a plethora of different nanolasers and related systems. In this sense, Taflove's results[21] were reproduced for testing the methodology. As a first step, the time domain of the system without gain is studied to describe the cavity. This study is shown in figure 4.

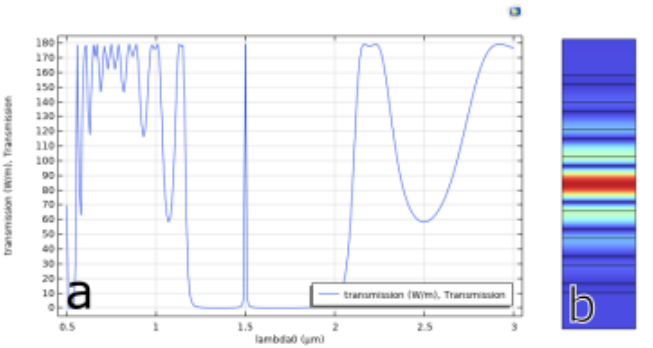

FIG. 4: a) transmission spectra of the mirror with the defect in the middle. **b)** Electric field amplitude profile of the mode of 1.5 μm.

Note that the DBR produce near null transmission around a very fine mode centred at 1.5 μm; far away, there are modes of low transmission. This fine localized mode corresponds to the defect, which will be responsible for lasing. The electric field is concentrated in the defect; thus, it will favour the stimulated emission.

The main result aimed is to reproduce figure 5. This figure shows the evolution of the populations of the VCSEL, now with the gain model implemented.

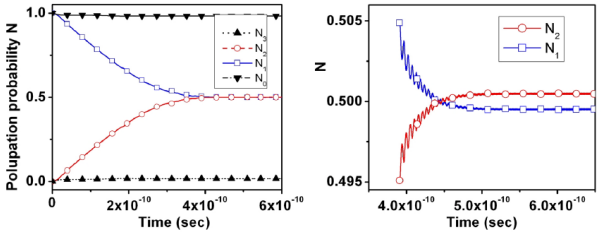

FIG. 5: Population probability, taken from reference 21

As the reference preclude saying explicitly the pump intensities used, we simulated several times to find one that can be suitable for this. Another issue is that the particular point where the populations are registered may not be the same. In this work, the chosen point is the upper border of the gain media for meshing reasons; in reference 21 the location of the point is not reported.

Figure 6 shows two simulations with different pumping amplitudes. In panel a) the pump is insufficient to produce the population inversion for $6\ 10^{-10} s$ and in panel b) the pump seems to be more intense than in the reference: the population inversion is reached before. The corresponding pumping amplitudes can be considered as lower and upper bounds for the one reported in the reference.

In figure 6c, there is Fourier transformed electric field amplitude at the pump frequency and the frequency of the amplified mode. Note that the gain media transformed the mode completely, compared with figure 4b. Now the field is more concentrated above the mirror, suggesting that the mode is no anymore localized, but it is propagating vertically.

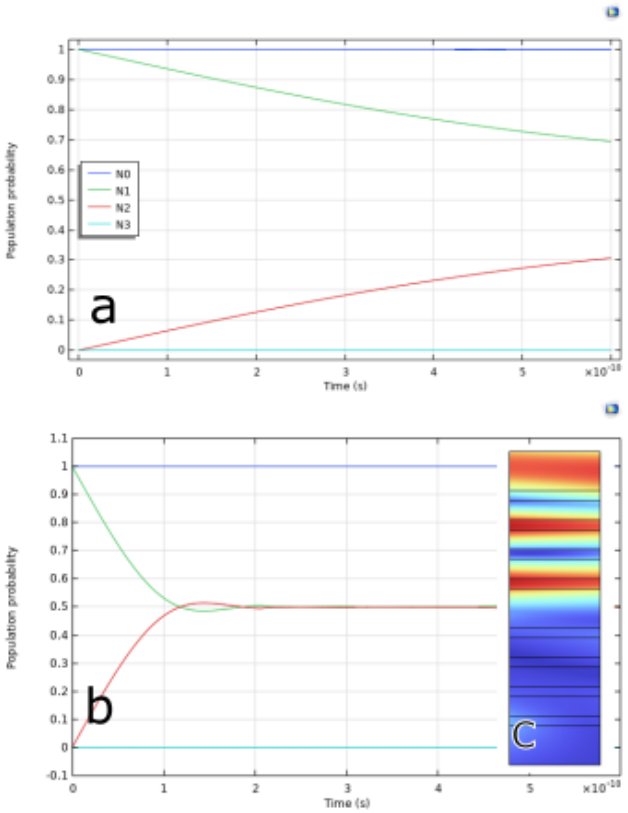

Fig. 6: Population probabilities at different pumping amplitudes **a)** $E_0 = 10^5 V/m$. **b)** $E_0 = 3\ 10^5 V/m$. **c)** Electric field amplitude profile of the mode of 1.5 μm, pumping amplitude same as b).

V. CONCLUSIONS

A. Perspectives

This work paves the way for implementing a whole family of models with an arbitrary number of levels and electrons and different transitions. This feature is essential in describing atomic transitions and mixes of atoms or molecules.

Moreover, the Rabi oscillations can be considered by adding a term in equations 21 and 22. These oscillations describe the phenomenon of strong coupling; this is the modification that the intense electromagnetic fields have over the electronic structure of the Dye.

The implementation in COMSOL also allows studying another physics coupling for realistic devices, for example, the possibility of including a fluidic for the dissolved Dyes. Also, to study the degradation of the molecules due to the action of the laser. The photo-thermal effect can also be implemented, and it is vital for microchip laser; the heating can produce deformation of the device, which can also be studied in COMSOL.

B. Conclusions

For this master thesis it was boarded the dye laser physics. The main goal of this work is to bring a consolidated model from the FDTD to the finite element method. This four levels two electrons model, implemented in one of the most popular software for photonics[4], now is available in COMSOL. This new implementation allows studying the phenomena further, linking it with other related physics.

COMSOL has a built-in model for the gain media in semiconductors; this work is an antecedent for expanding towards discretized energy states. Dyes can be in the liquid state, providing the possibility to interchange the gain media and tune its refractive index with the solvent without changing or dismantling the rest of the device. The broad emission spectra of these molecules can be an advantage in designing the pulse profile and tuning the output frequency.

A particular photonic example of nano-DyL was considered, but the overall achievement is beyond the particular VCSEL studied; it is constructing a method for studying complex physics with many implementations and applications. The difficulties of this work were mainly the long time of simulations and the lack of some particular data in the reference to reproduce. These difficulties were sorted, and now the way is paved to study new nanolasers and SPASERs within the multiphysics frame.

ACKNOWLEDGMENTS

The author wants to thank all the teachers of the master MUCOM for being excellent guides and support in this formative stage. Particularly to the tutor of this master thesis Emilio Ruiz Reyna for his patience and compromise. Also, to his research group for sharing the wave optics module licence. Also to Enrique Moreno Pérez who offered the workstation to perform the simulations.

REFERENCES

[1] Passarelli, N., Bustos-Marún, R. A., & Coronado, E. A. (2016). Spaser and optical amplification conditions in gold-coated active nanoparticles. The Journal of Physical Chemistry C, 120(43), 24941-24949.

[2] Passarelli, N., Bustos-Marún, R., & Depine, R. (2019). Lasing conditions of transverse electromagnetic modes in metallic-coated micro-and nanotubes. The Journal of Physical Chemistry C, 123(20), 13015-13026.

[3] Prelat, L., Cuevas, M., Passarelli, N., Marún, R. B., & Depine, R. (2021). Spaser and optical amplification conditions in graphene-coated active wires. JOSA B, 38(7), 2118-2126.

[4] Lumerical inc.

[5] Hecht, J. (2010). A short history of laser development. Applied optics, 49(25), F99-F122.

[6] Hulicius, E., & Kubeček, V. (2013). Semiconductor lasers for medical applications. In Lasers for Medical Applications (pp. 222-250). Woodhead Publishing.

[7] Normand, E., Howieson, I., McCulloch, M., & Black, P. (2006, September). Quantum Cascade Laser (QCL) based sensor for the detection of explosive compounds. In Optics and Photonics for Counterterrorism and Crime Fighting II (Vol. 6402, p. 64020G). International Society for Optics and Photonics.

[8] Moloney, J. V., & Laurain, A. (2018). Optically pumped semiconductor lasers. In Encyclopedia of Modern Optics (pp. 280-289). Elsevier.

[9] Pavlov, S. G., Zhukavin, R. K., Shastin, V. N., & Hübers, H. W. (2013). The physical principles of terahertz silicon lasers based on intracenter transitions. physica status solidi (b), 250(1), 9-36.

[10] William T. Silfvast, Encyclopedia of Physical Science and Technology, 2003

[11] Abramczyk, H. (2005). Introduction to laser spectroscopy. Elsevier.

[12] Azzam, S. I., Kildishev, A. V., Ma, R. M., Ning, C. Z., Oulton, R., Shalaev, V. M., ... & Zhang, X. (2020). Ten years of spasers and plasmonic nanolasers. Light: Science & Applications, 9(1), 1-21.

[13] Ma, R. M., & Oulton, R. F. (2019). Applications of nanolasers. Nature Nanotechnology, 14(1), 12-22.

[14] Berini, P., & De Leon, I. (2012). Surface plasmon–polariton amplifiers and lasers. Nature photonics, 6(1), 16-24.

[15] Kristanz, G. V., Arnold, N., Kildishev, A. V., & Klar, T. A. (2018). Power balance and temperature in optically pumped spasers and nanolasers. ACS photonics, 5(9), 3695-3703.

[16] Plotz, G. A., Simon, H. J., & Tucciarone, J. M. (1979). Enhanced total reflection with surface plasmons. JOSA, 69(3), 419-422.

[17] Yang, A., Hoang, T. B., Dridi, M., Deeb, C., Mikkelsen, M. H., Schatz, G. C., & Odom, T. W. (2015). Real-time tunable lasing from plasmonic nanocavity arrays. Nature communications, 6(1), 1-7.

[18] Tanizawa, M., Takahashi, R., Maruyama, T., & Iiyama, K. (2015, October). Pulsed oscillation of organic dye (Coumarin6) VCSEL excited by blue LD. In 2015 20th Microoptics Conference (MOC) (pp. 1-2). IEEE.

[19] Zhang, W., Yan, Y., Gu, J., Yao, J., & Zhao, Y. S. (2015). Low Threshold Wavelength Switchable Organic Nanowire Lasers Based on Excited State Intramolecular Proton Transfer. Angewandte Chemie, 127(24), 7231-7235.

[20] Ning, S., Wu, Z., Dong, H., Ma, L., Jiao, B., Ding, L., ... & Zhang, F. (2016). The enhanced random lasing from dye-doped polymer films with different-sized silver nanoparticles. Organic Electronics, 30, 165-170.

[21] Chang, S. H., & Taflove, A. (2004). Finite-difference time-domain model of lasing action in a four-level two-electron atomic system. Optics express, 12(16), 3827-3833.